ORIGINAL PAPER

Measurement methods and variability assessment of the Norway spruce total leaf area: implications for remote sensing

Lucie Homolová · Petr Lukeš · Zbyněk Malenovský · Zuzana Lhotáková · Věroslav Kaplan · Jan Hanuš

Abstract Estimation of total leaf area (LA_T) is important to express biochemical properties in plant ecology and remote sensing studies. A measurement of LA_T is easy in broadleaf species, but it remains challenging in coniferous canopies. We proposed a new geometrical model to estimate Norway spruce LA_T and compared its accuracy with other five published methods. Further, we assessed variability of the total to projected leaf area conversion factor (CF) within a crown and examined its implications for remotely sensed estimates of leaf chlorophyll content (C_{ab}). We measured morphological and biochemical properties of three most recent needle age classes in three vertical canopy layers of a 30 and 100-year-old spruce stands. Newly introduced geometrical model and the parallelepiped model predicted spruce LA_T with an error <5 % of the average needle LA_T, whereas two models based on an elliptic approximation of a needle shape underestimated LA_T by up to 60 %. The total to projected leaf area conversion factor varied from 2.5 for shaded to 3.9 for sun exposed needles and remained invariant with needle age class and forest stand age. Erroneous estimation of an average crown CF by 0.2 introduced an error of 2–3 μg cm^{-2} into the crown averaged C_{ab} content. In our study, this error represents 10–15 % of observed crown averaged C_{ab} range (33–53 μg cm^{-2}). Our results demonstrate the importance of accurate LA_T estimates for validation of remotely sensed estimates of C_{ab} content in Norway spruce canopies.

Keywords Chlorophyll content · Conversion factor · *Picea abies* · Projected leaf area · Remote sensing · Total leaf area

L. Homolová (✉)
Laboratory of Geo-Information Science and Remote Sensing, Wageningen University, Droevendaalsesteeg 3, 6708 PB Wageningen, The Netherlands
e-mail: lucie.homolova@wur.nl; lucie.homolova@gmail.com

L. Homolová · Z. Malenovský
Remote Sensing Laboratories, Department of Geography, University of Zürich, Winterthurerstrasse 190, 8057 Zurich, Switzerland
e-mail: zbynek.malenovsky@geo.uzh.ch; zbynek.malenovsky@utas.edu.au

P. Lukeš · V. Kaplan · J. Hanuš
Global Change Research Centre, Academy of Sciences of the Czech Republic, Bělidla 986/4a, 60300 Brno, Czech Republic
e-mail: lukes.p@czechglobe.cz

V. Kaplan
e-mail: kaplan.v@czechglobe.cz

J. Hanuš
e-mail: hanus.j@czechglobe.cz

Z. Malenovský
School of Geography and Environmental Studies, University of Tasmania, Private Bag 76, Hobart 7001, Australia

Z. Lhotáková
Department of Experimental Plant Biology, Faculty of Science, Charles University in Prague, Viničná 5, Prague, Czech Republic
e-mail: lhotakova@natur.cuni.cz

Introduction

Measurements and monitoring of forest structural and biochemical properties (e.g., leaf area index, leaf foliar pigment, nitrogen or water content) and physiological processes (e.g., gas exchange, photosynthesis) are important for the understanding of forest carbon sequestration (Luyssaert et al. 2007). Field measurements of forest

properties and processes are usually spatially and timely limited, labor demanding particularly in complex canopies such as mixed boreal or tropical forests. Thus, field measurements become impractical for large-scale applications. Emerging remote sensing (RS) imaging spectroscopy (often referred to as hyperspectral RS) has a great potential for regular monitoring of forest properties and processes at larger spatial scales (Kokaly et al. 2009; Rautiainen et al. 2010; Ustin et al. 2004). Currently, imaging spectroscopy data have been used to estimate leaf and canopy biochemical properties such as chlorophyll (Zarco-Tejada et al. 2004; Malenovský et al. 2006; Moorthy et al. 2008), nitrogen (Huber et al. 2008; Schlerf et al. 2010) and water content (Koetz et al. 2004; Clevers et al. 2010), canopy structural properties such as leaf area index (Fernandes et al. 2004), and eco-physiological processes such as mapping of net primary productivity (Ollinger and Smith 2005). Successful calibration and validation of the RS methods, however, depend on accurate and reliable field measurements of canopy biochemical properties that are often expressed at leaf area basis. While estimation of leaf area of broadleaf species is straightforward, it is a challenging task for non-flat coniferous needles. In case of conifers, total leaf area (LA_T) or hemisurface leaf area ($LA_H = \frac{1}{2}LA_T$) seems to be a more appropriate expression for gas exchange or photosynthesis-related studies than projected leaf area (LA_P), as stomata are located all around the needle surface (Smith et al. 1991).

The LA_T for broadleaf species is computed as two times LA_P, which can easily be measured by planimeters, desktop scanners, or leaf area meters (Beerling and Fry 1990). These techniques can be used to measure LA_P of coniferous species, but they are not suitable for LA_T (or LA_H) measurements due to the three-dimensional shape of needles. Needle LA_T has been determined by a volume displacement method (Johnson 1984) or from absorbance measurements of entire shoots (Serrano et al. 1997), but both methods are used rarely. More frequently, needle LA_T is computed from an approximation of the needle shape by a simple geometrical primitive (Sellin 2000; Niinemets and Kull 1995). Pine needles can be represented as half-cylinders or half-ellipsoids (Svenson and Davies 1992), spruce needles are usually modeled as parallelepipeds or ellipsoids (Sellin 2000). Dimensions of geometrical primitives are based on directly measurable morphometric variables, such as needle length and diameter. For example, Perterer and Körner (1990) proposed a complex model based on 9 different measures for spruce and 12 for pine needles, which significantly limits its practical use in forest research. Nevertheless, a detailed and accurate needle geometrical model is fundamental for developing simpler, feasible, but still reliable, methods to estimate LA_T of coniferous species.

Once LA_T is accurately determined, a conversion factor (CF) between LA_T and LA_P can be derived and used to estimate LA_T from easily measureable LA_P. Conversion factor is species specific, but it also varies within a canopy of the same species due to changing irradiance inside a canopy (Niinemets and Kull 1995; Sellin 2000). The characteristic organization of branches and shoots in coniferous canopies produces a heterogeneous radiation regime in a canopy vertical profile (Špunda et al. 1998; Chmura and Tjoelker 2008; Waring 1983). For example lower parts of a young spruce canopy can receive only about 10 % of irradiance when compared to the top of the canopy (Kalina et al. 2001). Light availability modulates leaf morphological properties (Hallik et al. 2009; Bond et al. 1999; Niinemets 2007); the shaded needles are usually more flat compared to sun exposed needles with more circular or rhomboidal cross-section (Cescatti and Zorer 2003). Usability of CF for LA_T estimation is, therefore, conditioned by understanding its variability between and within individual tree crowns.

Taking the advantage of high resolution digital photography and computer image processing techniques, the first objective of this study was to propose an accurate geometrical model to estimate LA_T of Norway spruce needles and compare it with five previously published LA_T estimating methods. The second objective was to investigate variability of the total to projected leaf area conversion factor (CF) taking into account three sources of variability: (1) needle position within a crown vertical profile, (2) needle age, and (3) canopy structure due to different forest stand age. Finally, the third objective was to quantify the influence of biased LA_T measurements on the estimation accuracy of crown averaged biochemical properties, which are being used for calibration and validation of remote sensing derived products.

Materials and methods

Study area and needle sampling

Morphological and biochemical properties of Norway spruce needles were analyzed for needle samples collected at the Bílý Kříž experimental research site (Moravian–Silesian Beskydy Mts. at the eastern part of the Czech Republic bordering with Slovakia; 18.53°E, 49.50°N, mean altitude of 880 m a.s.l.). The microclimatological conditions of the site are described in Urban et al. (2007).

Two montane Norway spruce (*Picea abies* (L.) Karst) forest stands of different age and structure were selected for this experiment: a 30-year-old regular plantation (further referred to as the "immature" stand), and an about 100-year-old stand (further referred to as the "mature"

stand), both growing on a moderate slope (13°) with S–SE orientation. In 2006, the average tree height was 12.5 m in the immature and 40 m in the mature stand, the average diameter at breast height was 14 and 53 cm, respectively, the canopy density was about 1,400 and 160 trees ha^{-1}, respectively, and the approximate stand area was 7.5 and 2.5 ha, respectively.

Ten immature and 20 mature representative trees were selected for the needle sampling. Double number of mature trees was considered, because we expected higher variability in needle morphological and biochemical properties due to a larger structural heterogeneity of the mature stand. One branch was collected from the upper (sun exposed zone, E); middle (transition zone, T); and bottom (sun shaded zone, S) canopy layer to capture varying irradiation conditions inside the canopies. From each branch, the last three needle age classes were sampled resulting in nine needle samples per tree. About 5–7 representative and visually healthy shoots (i.e., the annual growth segments) per needle age class were selected and about 30 individual needles were randomly sampled from the central part of shoots. Each needle sample was divided into three subsets including about ten needles each: the first subset was used for estimation of needle LA_T and LA_T/LA_P conversion factor, the second subset for needle water content and specific leaf area, and the third subset for photosynthetic pigment analysis. In total, we collected three times 270 needle samples.

Posterior statistical assessment of the optimal sample size using the Power t test (Erdfelder et al. 1996) indicated a minimum sample size of 21 trees to assess the total variance of CF, which was exceeded with total of 30 trees sampled.

Estimation of needle LA_T and CF

The needles from the first subset for LA_T estimation were kept deep-frozen until the laboratory processing. Individual needle samples were first scanned on a desktop scanner to measure LA_P and then five needles were randomly selected for further processing (preceding analysis indicated that 5 needles is sufficient to obtain LA_T representative for the entire needle sample; results not shown). Five needles were scanned on a desktop double-lamp scanner to determine their individual LA_P and length along curvature (L). Then three cross-sections (approximately 100 μm thick) were obtained from the base, middle and top part of a needle using a hand microtome. Micrographs of cross-sections were acquired with the Canon EOS 450D digital camera, which was mounted on the Novex BT PL microscope. The micrographs were captured uncompressed with maximum possible resolution of 12 MPix to ensure high precision of image analysis. Perimeter and length of both the major (D_1) and the minor (D_2) diameters were measured automatically

for each cross-section using a self-developed image analysis procedure [combination of Python 2 and GNU (General Public Licence) Image Manipulation Program (GIMP, v. 2.6)].

The total leaf area of spruce needles was estimated using six methods. We proposed a new geometrical model for LA_T estimation of spruce needles (method I), which was based on the model of Perterer and Körner (1990). Our model approximated the spruce needle shape to three geometric primitives: two adjacent circular cone frustums, and a cone cap representing a tapered needle's top (Fig. 1). The total leaf area of a needle was calculated according to the following equation:

$$LA_T I = \frac{P_B + P_M}{2} L'_{B-M} + \frac{P_M + P_T}{2} L'_{M-T} + \frac{P_T L'_T}{2}, \quad (1)$$

where P_B, P_M, and P_T are the measured perimeters of three cross-sections placed at the base ($_B$), middle ($_M$) and top ($_T$) of a needle, respectively. L'_{B-M} is a slant height of the cone frustum between the base and the middle cross-sections calculated from the measured cone height L_{B-M} as $L'_{B-M} = \sqrt{L_{B-M}^2 + (P_B/2\pi - P_M/2\pi)^2}$. L'_{M-T} is a slant height of the cone frustum between the middle and the top cross-section calculated analogous to $L'_{B-M} L'_T$ is a slant height of a cone cup calculated as $L'_T = \sqrt{L_T^2 + (P_T/2\pi)^2}$. We assumed that $L_T = 1.5$ mm, $L_{B-M} = L_{M-T}$ and the sum of the three lengths was equal to the total needle length measured along the curvature of the needle central axis (L) as illustrated at Fig. 1b.
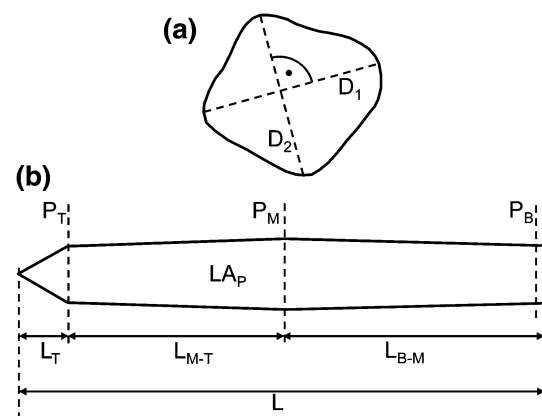

Fig. 1 Geometrical model developed in this study to calculate total leaf area of Norway spruce needles and its inputs: (a) needle cross-section and its major (D_1) and minor (D_2) diameters, (b) schematic position of three cross-sections (P_T, P_M, P_B are perimeters of a cross-section at the *top*, *middle*, and *bottom* part of a needle, respectively; L_{B-M}, L_{M-T} are lengths of segments between two cross-sections assuming that $L_{B-M} = L_{M-T}$; L_T is height of cone cap, which was approximately 1.5 mm; L is total needle length measured along the curvature of the needle central axis; LA_P is projected leaf area of a needle)

The other five methods for estimation of needle LA_T were previously published in scientific literature. More details on methods II–V can be found in Sellin (2000) and on method VI in Pokorný (2002). Here, we provide only the final formulas and the variables are explained at Fig. 1:

Method II: A needle side approximated to a parallelepiped:

$$LA_T II = 2L\sqrt{D_1^2 + D_2^2} \qquad (2)$$

Method III: A needle side approximated to an ellipse:

$$LA_T III = \frac{\pi L\sqrt{D_1^2 + D_2^2}}{2} \qquad (3)$$

Method IV: A needle approximated to an ellipsoid:

$$LA_T IV = \pi \sqrt[3]{D_1^2 D_2^2 L^2} \qquad (4)$$

Method V: A needle side approximated to a rectangle with tapering ends to a half-ellipse:

$$LA_T V = \frac{4rL\sqrt{D_1^2 + D_2^2} + (1-r)\pi L\sqrt{D_1^2 + D_2^2}}{2} \qquad (5)$$

(r is the relative length of the rectangular part of a needle and it was equal to 0.75).

Method VI: CF derived as the ratio of the middle cross-section perimeter and major diameter:

$$LA_T VI = \frac{P_M}{D_1} LA_P \qquad (6)$$

Six LA_T estimating methods (Eq. 1–6) were compared at the individual needle level against the same reference ($\overline{LA_T}$). The reference total leaf area was calculated for 21 needles, which were selected across the entire sample pool to capture the variability of a needle shape. We took 9–15 cross-sections per needle, depending on its length, and calculated $\overline{LA_T}$ using the same principle as presented for method I (Eq. 1), but instead of two we integrated surface area of up to 14 cone frustums.

Finally, the conversion factor between total (method I) and projected (scanned) leaf area was calculated as a simple ratio: CF = LA_T / LA_P. We applied a three-way analysis of variance (ANOVA) at the significance level $\alpha = 0.01$ and with a prior normality test to analyze CF variability between and within spruce crowns considering three potential sources of CF variability: (1) needle position within a crown vertical profile, (2) needle age, and (3) forest stand age.

Measurement of needle biochemical properties and upscaling to a crown level

The second and the third needle subsets were used to analyze the following needle biochemical properties:

specific leaf area (SLA), water (C_w), chlorophyll $a + b$ (C_{ab}) and carotenoid (C_{xc}) content. Needles for SLA and C_w content determination were weighted immediately after clipping, stored in paper bags, dried in an oven at 60 °C for 48 h, and weighted again after drying. Needles for photosynthetic pigments (C_{ab} and C_{xc}) were kept in deep freeze and dark until being processed in a laboratory. Pigments were extracted according to the method of Porra et al. (1989) using the dimethylformamide solvent and the pigment concentration was determined spectrophotometrically according to the equations of Wellburn (1994). Following the terminology proposed by Datt (1998), we define constituent concentration as mass fraction per unit dry leaf mass (mg g^{-1}) and constituent content as mass fraction per unit leaf area (mg cm^{-2}). Equation 7 shows the conversion between concentration and content of a constituent X (C_w, C_{ab} or C_{xc}) using specific leaf area [SLA$_H$, the ratio of hemisurface leaf area (cm^2) to the corresponding dry mass weight (g)].

$$X[\text{mg cm}^{-2}] = \frac{X[\text{mg g}^{-1}]}{SLA_H[\text{cm}^2 \text{ g}^{-1}]} \qquad (7)$$

The upscaling from the leaf to the crown level was done by simply averaging nine values of leaf level biochemical content per tree (i.e., combination of needle samples from three crown vertical layers and three needle age classes). The mean value per crown is hereafter referred to as "crown averaged content". We selected this simple upscaling approach, because it is often used in remote sensing studies (e.g., Zarco-Tejada et al. 2004; Huber et al. 2008; Schlerf et al. 2010).

In order to evaluate the effect of LA_T estimation on crown averaged biochemical content of SLA, C_w, C_{ab} and C_{xc}, first, we calculated crown averaged biochemical content using six LA_T estimating methods (Eqs. 1–6). SLA$_H$ computed from six different LA_T values served as the basis for conversion from needle biochemical concentrations to contents (Eq. 7). Second, we considered a theoretical case, where needle biochemical concentration (mg g^{-1}) and corresponding LA_P are known, but a sample LA_H is unknown. Missing LA_H was then calculated as $LA_P \times$ CF $\times$ 0.5, where LA_P is the measured projected leaf area of a sample and CF is a theoretical value of the total to projected leaf area conversion factor. The theoretical CF varied within a physically meaningful range from 2 (flat needles) to 4 (square shaped needles) with steps of 0.2, while assuming a constant theoretical CF value for entire crown vertical profile. Once again, we computed crown averaged biochemical content (X_{CF}) as a simple average of nine needle biochemical contents, but this time using the theoretical CF to estimate a sample LA_H. X_{CF} was then compared with crown averaged biochemical content
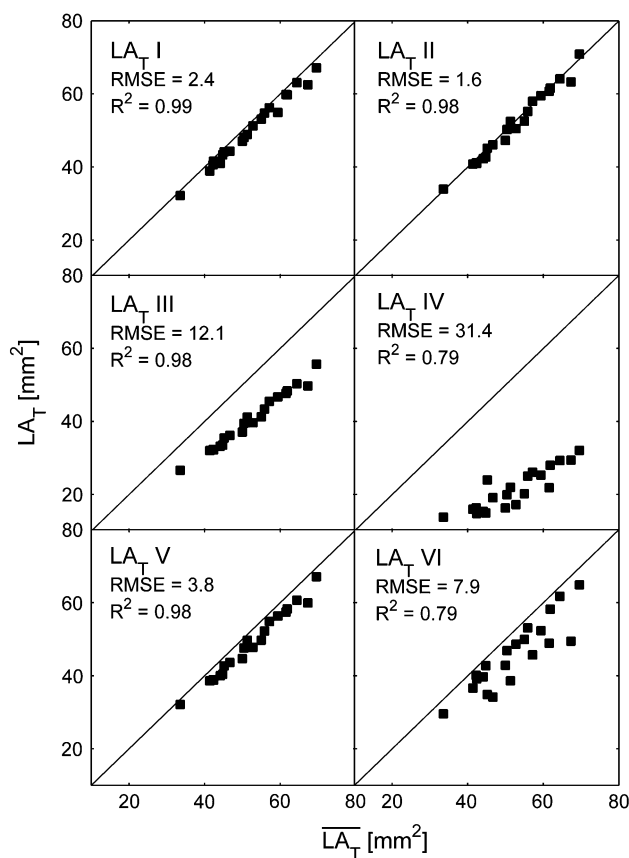
Fig. 2 Comparison of six methods for estimation of total leaf area (Eq. 1–6) for individual spruce needles ($n = 21$) with the reference method ($\overline{LA_T}$). Root mean square error (RMSE) between each method and the reference, and coefficient of determination (R^2) are indicated for each method

(X_{REF}), based on the LA_T estimating method I (Eq. 1), using root mean square error (RMSE):

$$RMSE = \sqrt{\frac{1}{n}\sum_{i=1}^{n}\left(X_{i,CF} - X_{i,REF}\right)^2}, \tag{8}$$

where n is the number of trees.

Results

Accuracy of LA_T estimating methods

The accuracy of six LA_T estimating methods was assessed at the level of individual needles (in total 21 needles selected from the entire sample pool) by comparing all methods against one reference (Fig. 2). The reference total leaf area ($\overline{LA_T}$) was calculated from 9 to 15 cross-sections taken along the needle length using similar principle as presented in Eq. 1. The average total area of a single needle was 52.2 (± 9.5) mm^2. Detailed cross-sections analysis showed that the minor diameter of needle
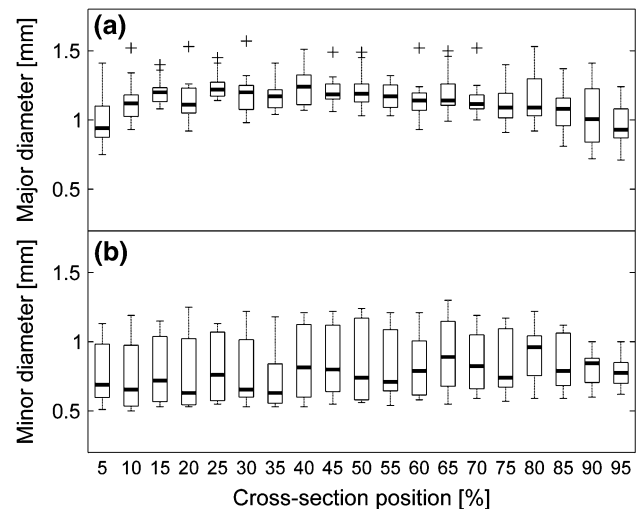

Fig. 3 Changes on needle cross-section major diameter (**a**) and minor diameter (**b**) along the needle length. The position of needle cross-section (x axis) is expressed in relative units, where 0 % refers to the *needle base* and 100 % to the *needle top*. *Central line* in a box represents median, box height represents 50 % of the data (interquartile range), whiskers represent the minimum and the maximum values, and crosses represent outliers (when observed values exceeded 1.5 times the interquartile range)

cross-sections is almost invariant along the entire needle length, whereas the major diameter decreases towards the needle ends (Fig. 3). The coefficient of determination (R^2) between the LA_T estimating methods and the reference was generally high, varying between 0.79 and 0.99. Methods I and II provided accurate estimates of LA_T, R^2 was higher than 0.98 and RMSE was equal to 2.4 and 1.6 mm^2, respectively. In both cases, the relative RMSE was smaller than 5 % of the average needle LA_T. Method III, which modeled needle side as an ellipse, and method IV, which modeled needle as an ellipsoid, systematically underestimated LA_T, with RMSE of 12.1 and 31.4 mm^2, respectively. Relative RMSE was up to 60 % of the average needle LA_T.

Variability of total to projected leaf area conversion factor for method I

The sample-specific conversion factor (CF) computed between LA_T (method I, Eq. 1) and scanned LA_P varied from 2.5 to 3.8 (95th percentile). We examined three sources of CF variability: (1) needle position within a crown vertical profile, (2) needle age, and (3) forest stand age (Fig. 4; Table 1). CF of the sun exposed needles was higher than the CF of transition and shaded needles ($p \leq 0.01$). The mean values of CF were 3.47 (sun exposed needles), 3.18 (transition), and 2.84 (shaded needles) for the immature canopy and 3.44, 2.90, and 2.85, respectively, for the mature canopy. We did not find any statistically
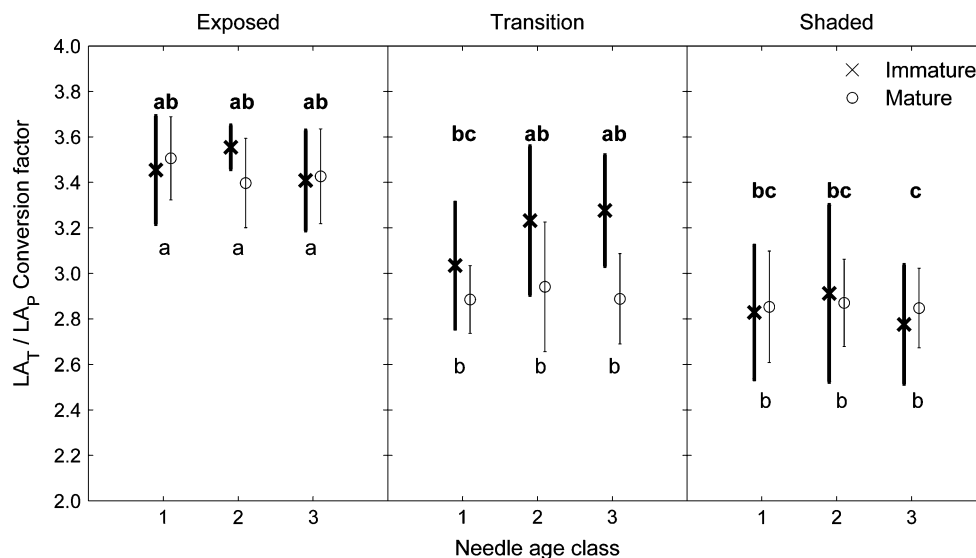
Fig. 4 Total to projected leaf area conversion factor (CF) of two experimental Norway spruce stands, immature (*times symbol*) and mature (*open circle*). The symbols represent mean values per needle category (combination of three needle age classes and three canopy vertical layers—sun exposed, transition and shaded). The whiskers represent the two-sided SD. *Equal letters* above (immature stand) and below (mature stand) data points connect homogeneous groups within each forest stand, i.e., statistically insignificant differences between data groups at $p \leq 0.01$ (ANOVA, Tukey's post hoc test)

significant differences among three investigated needle age classes. The CF was nearly invariant between the immature and mature stand, except the transition canopy level, where CF of mature trees was lower compared to immature trees.

Finally, the CF was closely related to the ratio of the middle cross-section perimeter (P_M) and its major diameter (D_{1M}), with R^2 equal to 0.73, and thus CF could be reasonably modeled as:

$$CF = 0.47 \left(\frac{P_M}{D_{1M}} \right) + 1.31 \tag{9}$$

Impact of LA_T on upscaling of foliar biochemistry from leaf to crown level

At the needle level, biochemical concentration and content varied with needle age and canopy vertical position as summarized in Table 1. Pigment concentration (i.e., normalized by the dry mass) increased with increasing needle age and shadowing, whereas content (i.e., normalized by LA_H according to Eq. 7) increased only with needle age and remained nearly invariant among canopy vertical layers. Needle water content did not vary with needle age, but the typically sun shaded needles had lower C_w content than the exposed needles. Specific leaf area, the ratio between needle LA_H and the dry mass, was the most variable needle property. It varied between 30 and 140 cm^2 g^{-1} and it decreased with needle age and increased with increasing shadowing inside the canopy.

At the crown level, we first examined the influence of different LA_T estimating methods on the crown averaged

biochemical content (Fig. 5). Second, we examined whether the crown averaged biochemical content is sensitive towards biased LA_T estimates due to variable CF (Fig. 6). Although we analyzed all biochemical properties, for brevity, we present results only for the chlorophyll content, because it is one of the most frequently studied vegetation property by remote sensing (Ustin et al. 2009; le Maire et al. 2004) and all biochemical properties showed similar response to different LA_T estimating methods.

An average crown averaged C_{ab} was equal to 39 μg cm^{-2} for the immature and 42 μg cm^{-2} for the mature spruce trees and it varied between 33 and 53 μg cm^{-2} (values based on LA_T estimations using our adjusted geometrical model, i.e., method I, hereafter used as the reference crown averaged C_{ab}). Figure 5 shows how different LA_T estimating methods yielded different crown averaged C_{ab} values. Methods II, V and VI, which estimated LA_T similar to our geometrical model (method I) produced crown averaged C_{ab} within the similar range (33–53 μg cm^{-2}). Methods III and IV, which underestimated LA_T, overestimated crown averaged C_{ab} up to 1.5 times. For illustration purposes, we also show that the crown averaged C_{ab} normalized by LA_P is about 50 % higher than C_{ab} normalized by LA_T (cf. the first and the last box of Fig. 5).

The small case study with the theoretical CF, which varied between two and four with steps of 0.2, demonstrated how crown averaged C_{ab} content is sensitive to potentially biased LA_T estimates. Crown averaged chlorophyll content was exponentially increasing with

Table 1 Morphological and biochemical properties of Norway spruce needles obtained from sampling of 10 immature and 20 mature trees from three canopy vertical layers (exposed, transition and shaded) and three most recent needle age classes (1, most recent; 2, last year; 3, two-year-old needles)

	Age class	Immature			Mature		
		Exposed	Transition	Shaded	Exposed	Transition	Shaded
Needle length (mm)	1	15.9 ± 1.2	16.3 ± 2.6	13.3 ± 2.0	15.8 ± 2.2	17.7 ± 2.0	17.1 ± 2.5
	2	16.5 ± 1.1	15.3 ± 1.7	14.8 ± 1.4	18.1 ± 2.2	16.6 ± 2.5	16.0 ± 2.8
	3	18.8 ± 1.8	16.9 ± 2.3	17.1 ± 2.4	17.3 ± 2.5	18.4 ± 2.7	17.6 ± 2.9
Major diam. D_1 (mm)	1	1.19 ± 0.06	1.16 ± 0.07	1.07 ± 0.10	1.29 ± 0.14	1.13 ± 0.07	1.10 ± 0.09
	2	1.23 ± 0.09	1.18 ± 0.04	1.15 ± 0.05	1.38 ± 0.10	1.12 ± 0.08	1.07 ± 0.08
	3	1.26 ± 0.07	1.22 ± 0.04	1.16 ± 0.06	1.25 ± 0.13	1.18 ± 0.10	1.11 ± 0.09
Minor diam. D_2 (mm)	1	1.04 ± 0.12	0.67 ± 0.13	0.61 ± 0.25	1.10 ± 0.07	0.64 ± 0.08	0.54 ± 0.06
	2	1.08 ± 0.09	0.84 ± 0.15	0.61 ± 0.17	1.18 ± 0.13	0.66 ± 0.10	0.64 ± 0.11
	3	1.03 ± 0.15	0.88 ± 0.14	0.67 ± 0.19	1.19 ± 0.09	0.59 ± 0.05	0.55 ± 0.06
LA_T/LA_P CF (–)	1	3.46 ± 0.23	3.09 ± 0.25	2.83 ± 0.27	3.51 ± 0.18	2.89 ± 0.15	2.85 ± 0.24
	2	3.55 ± 0.09	3.25 ± 0.29	2.92 ± 0.37	3.40 ± 0.19	2.94 ± 0.28	2.87 ± 0.19
	3	3.41 ± 0.21	3.30 ± 0.23	2.77 ± 0.24	3.43 ± 0.20	2.89 ± 0.19	2.85 ± 0.17
C_{ab} conc. (mg g^{-1})	1	1.47 ± 0.28	2.33 ± 0.65	3.29 ± 0.96	1.86 ± 0.35	2.68 ± 0.52	2.77 ± 0.40
	2	2.06 ± 0.32	2.63 ± 0.48	3.11 ± 0.58	2.36 ± 0.49	3.15 ± 050	3.30 ± 0.48
	3	2.21 ± 0.45	2.57 ± 0.33	3.38 ± 0.54	2.23 ± 0.47	3.46 ± 0.51	3.76 ± 0.52
C_{ab} content (μg cm^{-2})	1	23.7 ± 4.5	32.3 ± 12.3	38.7 ± 6.6	32.2 ± 6.8	32.7 ± 3.3	30.1 ± 4.0
	2	40.4 ± 6.2	41.3 ± 8.4	48.2 ± 9.0	48.8 ± 9.6	43.8 ± 7.4	41.0 ± 5.8
	3	43.0 ± 8.4	43.4 ± 5.5	50.4 ± 13.6	46.6 ± 12.5	49.2 ± 8.2	45.2 ± 5.6
C_{xc} conc. (mg g^{-1})	1	0.26 ± 0.05	0.36 ± 0.12	0.46 ± 0.15	0.30 ± 0.05	0.36 ± 0.06	0.37 ± 0.05
	2	0.35 ± 0.06	0.41 ± 0.07	0.46 ± 0.09	0.38 ± 0.07	0.44 ± 0.07	0.46 ± 0.07
	3	0.37 ± 0.08	0.42 ± 0.05	0.51 ± 0.06	0.38 ± 0.07	0.50 ± 0.07	0.54 ± 0.07
C_{xc} content (μg cm^{-2})	1	4.1 ± 0.8	5.0 ± 2.3	4.3 ± 1.0	5.2 ± 0.9	4.4 ± 0.4	4.1 ± 0.5
	2	6.9 ± 1.1	6.4 ± 1.1	5.6 ± 1.6	7.8 ± 1.5	6.2 ± 1.1	5.8 ± 0.9
	3	7.3 ± 1.4	7.1 ± 0.8	7.3 ± 1.9	7.8 ± 1.9	7.1 ± 1.3	6.5 ± 0.9
C_w conc. (g g^{-1})	1	0.59 ± 0.02	0.62 ± 0.02	0.63 ± 0.02	0.55 ± 0.02	0.61 ± 0.02	0.61 ± 0.03
	2	0.56 ± 0.02	0.59 ± 0.02	0.61 ± 0.03	0.53 ± 0.02	0.58 ± 0.05	0.57 ± 0.02
	3	0.56 ± 0.01	0.58 ± 0.01	0.61 ± 0.03	0.50 ± 0.03	0.56 ± 0.03	0.57 ± 0.03
C_w content (mg cm^{-2})	1	23.8 ± 1.6	22.8 ± 3.2	16.7 ± 2.4	22.0 ± 3.1	20.2 ± 5.8	17.9 ± 4.7
	2	25.1 ± 1.9	23.0 ± 3.4	19.3 ± 3.1	23.5 ± 3.0	19.0 ± 3.5	16.7 ± 3.0
	3	25.4 ± 2.7	23.3 ± 1.9	22.0 ± 5.5	21.2 ± 3.2	18.1 ± 2.6	16.4 ± 1.7
SLA_H (cm^2 g^{-1})	1	61.8 ± 3.3	74.2 ± 10.6	105.8 ± 24.9	58.7 ± 9.4	82.4 ± 15.3	91.0 ± 17.3
	2	51.3 ± 5.1	64.5 ± 8.5	82.7 ± 17.5	48.6 ± 5.2	73.1 ± 12.7	81.6 ± 13.1
	3	51.5 ± 4.7	59.6 ± 6.5	75.6 ± 23.2	48.7 ± 5.1	71.1 ± 10.2	83.8 ± 10.8

The values are presented as mean $\pm$ SD

decreasing theoretical CF (Fig. 6b). The smallest RMSE (Eq. 8) between the reference crown averaged C_{ab} and C_{ab} estimated using the theoretical CF was found for the value equal to 3.0 (Fig. 6a). The smallest RMSE agreed well with the mean measured conversion factor for the immature (CF = 3.2) and the mature (CF = 3.1) spruce crowns. Large errors up to 25 μg cm^{-2} in crown averaged C_{ab} were observed for the lower values of the theoretical CF (closer to flat needles). A bias of 0.2 from the true conversion factor introduced an error of 2–3 μg cm^{-2} in crown averaged C_{ab} estimates.

Discussion

Accuracy of LA_T estimating methods

Modeling a spruce needle using our new geometrical model (method I), parallelepipeds as a proxy of needle sides (method II), or parallelepipeds with half-elliptic tapering (method V) resulted in LA_T estimates closely comparable with the true reference $\overline{LA_T}$ (Fig. 2). Only methods I and II estimated LA_T of a single needle with relative RMSE <5 % of the average LA_T. According to
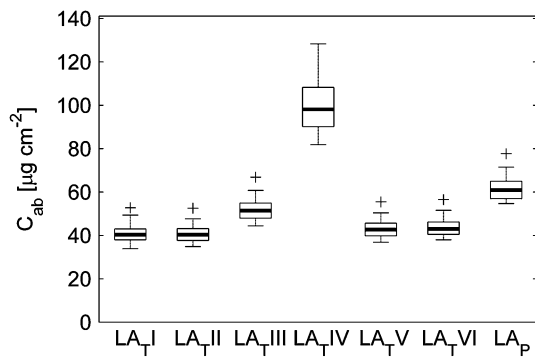
Fig. 5 Summary statistics of crown-averaged chlorophyll content for 30 Norway spruce trees. Six methods to estimate total leaf area (LA_T) and directly measured projected leaf area (LA_P) were used to express measured chlorophyll per leaf area. Detailed explanation of box plots can be found in the legend of Fig. 3
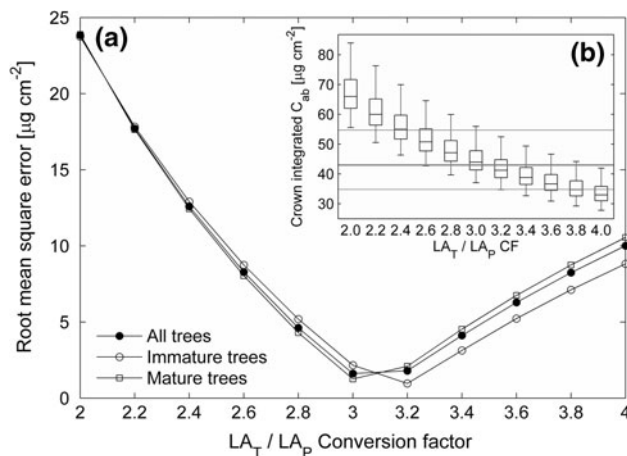

Fig. 6 (**a**) RMSE (Eq. 8) between crown averaged leaf chlorophyll (C_{ab}) content normalized by LA_H calculated using sample specific CF (based on the LA_T estimating method I) and theoretical CF (i.e., single value for entire crown vertical profile, which varies between 2 and 4 with steps of 0.2). The mean RMSE values were calculated for 30 Norway spruce crowns (*black dots*), i.e., 10 immature (*squares*), and 20 mature (*circles*). The inserted figure (**b**) demonstrates how crown-averaged C_{ab} decreases with increasing theoretical CF. *The gray thick line* represents the median and *two gray thin lines* indicate min.–max. range of the crown averaged content based on our LA_T estimating method I. Detailed explanation of box plots can be found in the legend of Fig. 3

study of Frey (as cited in Niinemets 1997), method II systematically underestimated real Norway spruce LA_T by 5–8 %, but we did not observe any systematic underestimation. Contrary to the accurate LA_T estimates by methods I and II, method III (needle sides modeled as an ellipse) and method IV (a needle modeled as an ellipsoid) systematically underestimated needle LA_T by 23 and 60 %, respectively. Similar result was reported by Sellin (2000), who modeled a needle shape as an ellipse, which underestimated spruce needle LA_P by up to 20 %. Our results

suggest that an elliptic approximation is not suitable for modeling Norway spruce needles, because it introduces unrealistic tapering starting already at the middle part of a needle. Analysis of needle cross-sections for computing the reference total leaf area ($\overline{LA_T}$) confirmed that the major and the minor cross-section diameters are nearly invariant for 75 % of the needle length and only the major diameter decreases towards needles' ends (Fig. 3). Thus, modeling Norway spruce needle shape as suggest by methods I, II and IV seems to be more suitable for LA_T estimation.

A reliable predictor of the total to projected leaf area CF seems to be the ratio between the middle cross-section perimeter and its diameter ($R^2 = 0.73$). The same approach uses method VI (Pokorný 2002) to estimate LA_T from LA_P, which was in reasonably good agreement with the reference $\overline{LA_T}$, as well as with our geometrical model method VI underestimated a single needle LA_T by <15 %.

Variability of total to projected leaf area conversion factor for method I

The values of total to projected leaf area CF varied from 2.5 to 3.8 (Fig. 4), which is in agreement with previously published CF values for various Norway spruce canopies. A CF between 2.3 and 3.1 (mean of 2.4) was observed for a 15-year-old experimental plantation in the Czech Republic (Pokorný 2002), 2.3–3.7 (median around 2.5) was observed for current-year needles of 12–32-year-old trees in Germany (Niinemets 1997), 3.0–3.3 (mean of 3.1) was observed for a 30-year-old forest in Estonia (Sellin 2000), or slightly higher CF values in the range of 3.0–4.0 (mean of 3.6) were observed for current-year needles of a 40-year-old plantation in Northern Sweden (Stenberg et al. 1999). Our results showed, nevertheless, higher CF values than the average CF presented by Pokorný (2002), who studied the same immature Norway spruce stand in 1999. He reported an average CF of 2.6, whereas mean of our CF measurements was equal to 3.2. The discrepancy can be attributed to different methodologies and possibly also to higher light availability due to increasing canopy openness with the time induced by natural disturbances and managed thinning.

The majority of the studies measuring the CF of Norway spruce were carried out on trees with an age less than 40 years and the results from those studies indicate that CF increases with increasing canopy age. In our study, we sampled trees in their mature age (around 100 years old) and we found that the average CF was almost equal to the one measured in the 30-year-old spruce canopy. Our results indicated that CF values of entirely sun exposed and shaded needles were not significantly different in both stands. Some differences in CF were observed in the transition

canopy vertical layer (Fig. 4), which can be characterized by more variable irradiation conditions. The needles from the transition zone of the mature canopy tended to have CF similar to shaded needles. This indicates that the transition needles of the mature trees were actually sampled deeper in the canopy, i.e., from locations with less available light, than the transition needles of the immature stand. A more accurate physical based delineation of canopy sampling positions, e.g., using measurements of incident radiation, might solve this mismatch and assure inter-comparability of needle samples collected from different forest stands.

The decreasing trend of CF in the canopy vertical profile is attributed to the decreasing light availability in the lower parts of the canopy. Lower CF values together with more horizontally oriented foliage result in larger foliar surface, which helps trees to improve the light harvesting capacity of shaded branches. Similar trend of decreasing CF with decreasing light availability has been reported for Central European Norway spruce by Niinemets (1997) and by Niinemets and Kull (1995), and for Silver fir dominated stands by Cescatti and Zorer (2003). Contrasting result, i.e., no trend between CF and light availability, was reported by Palmroth et al. (2002) for spruces growing in central Sweden. This independency can be attributed to the narrower crown habitus and typically more open canopies in higher latitudes, which ensure more equal distribution of light within the crown vertical profile. Furthermore, suppressed shade-tolerant Silver firs (Cescatti and Zorer 2003) and shade-intolerant Scots pines (Niinemets 2010) did not exhibit any clear trend either. This indicates that local ecological factors and tree social position play an important role in foliage adaptations towards varying irradiance intensities.

Finally, we did not observe significant differences in CF among three recent needle age classes, which is in agreement with results previously published by Sellin (2000).

Impact of LA_T on upscaling of foliar biochemistry from leaf to crown level

Leaf biochemical properties, such as chlorophyll and water, are in quantitative remote sensing studies often expressed per leaf area (Jacquemoud et al. 1996). Consequently, biochemical properties of non-flat spruce needles with a quadratic cross-section can significantly differ if being expressed against the projected or the total leaf area (Niinemets 2010 and Fig. 5 in this study). As demonstrated in Fig. 4, CF is decreasing with decreasing light availability inside the spruce canopies. Assuming a single, average CF value around 3.0 for the entire canopy profile, CF causes an overestimation of LA_T for shaded and an underestimation of LA_T for sun exposed needles. This error is further propagated into the measurements of biochemical content at the leaf level, as well as into crown averaged values. Based on Fig. 6a, erroneous estimation of the mean crown CF by 0.2 introduces already an error of 2–3 $\mu g\ cm^{-2}$ in crown averaged chlorophyll content. Considering that observed range of crown averaged C_{ab} was only 20 $\mu g\ cm^{-2}$ (i.e., it varied between 33 and 53 $\mu g\ cm^{-2}$), the error represents 10–15 % of the observed range. However, the variability of observed crown averaged C_{ab} was small as it can vary between 20 and 100 $\mu g\ cm^{-2}$ (Malenovský et al. 2006). The maximum RMSE due to erroneous estimation of the CF was up to 25 $\mu g\ cm^{-2}$. This error is even higher than the accuracy of common remote sensing methods estimating crown averaged chlorophyll content in coniferous canopies, which is usually around 10 $\mu g\ cm^{-2}$ (Malenovský et al. 2006; Zarco-Tejada et al. 2004; Moorthy et al. 2008).

Attention should be paid to methods of upscaling from the leaf biochemical properties to the crown or even canopy levels. In this study, we used simple averaging of leaf measurements, because it is the most frequent approach used in remote sensing studies investigating forest biochemical properties (e.g., Zarco-Tejada et al. 2004; Huber et al. 2008; Schlerf et al. 2010). Nevertheless, more sophisticated upscaling schemes, which would take into account real distribution of leaf biomass within the crown vertical profile, can likely provide more representative crown integrates. For example, Lukeš et al. (2009) combined the vertical distribution of leaf biomass and extinction of photosynthetically active radiation into a scaling scheme, which produced more realistic ground truth for validation of remotely sensed chlorophyll content of spruce crowns. Forthcoming upscaling studies should consider employing the rapidly developing methods of terrestrial and airborne laser scanning. Laser scanning enables mapping of 3D foliage distribution of individual tree crowns (van der Zande et al. 2006) and of complex forest stands (Morsdorf et al. 2010).

Conclusions

Two out of six evaluated LA_T estimating methods, our newly proposed geometrical model based on three needle cross-sections (method I) and the parallelepiped model (method II), predicted Norway spruce needle LA_T with an error <5 % of the average needle LA_T. Considering the overall feasibility of both methods, we can conclude that the parallelepiped model seems to be more suitable for an operational LA_T estimation in eco-physiology and applied remote sensing research, because it requires less inputs than the new geometrical model. Methods III and IV, which suggest an elliptic approximation of a needle shape, underestimated LA_T by up to 60 %, and thus are not suitable for prediction of spruce needle LA_T. The conversion

factor between total and projected leaf area (CF) was estimated with a reasonable accuracy ($R^2 = 0.73$) using the ratio between the needle perimeter and the major diameter of a cross-section taken from the middle of a needle. CF varied from 2.5 (shaded needles) to 3.8 (sun exposed needles). The variability of CF was mainly driven by the position of needles in the vertical canopy profile, or in other words by the decreasing irradiation in the lower canopy layers. Influence of the needle and the stand age on the CF variability was insignificant. Therefore, for future field measurements of CF we recommend sampling needles irrespective of their age (i.e., a mixed sample of several needle age classes), but taking into account several canopy vertical layers.

Since leaf area normalized biochemical properties (e.g., leaf chlorophyll and water content) of forest canopies can be estimated using the airborne and satellite imaging spectroscopy methods, representative and accurate field measurements are required for calibration and validation of the remote sensing methods. We demonstrated that crown averaged chlorophyll (C_{ab}) content normalized by LA_P is about 50 % higher than LA_T normalized C_{ab} content. Moreover, inaccurately estimated LA_T due to biased CF can introduce an error into crown averaged chlorophyll content reaching up to 25 $\mu g\ cm^{-2}$. If we consider a possible range of crown averaged C_{ab} between 20 and 100 $\mu g\ cm^{-2}$, the error can represent up to 30 % of the total C_{ab} range, which can seriously affect the reliability of remote sensing methods.

References

Beerling DJ, Fry JC (1990) A comparison of the accuracy, variability and speed of five different methods for estimating leaf area. Ann Bot 65(5):483–488

Bond BJ, Farnsworth BT, Coulombe RA, Winner WE (1999) Foliage physiology and biochemistry in response to light gradients in conifers with varying shade tolerance. Oecologia 120(2):183–192

Cescatti A, Zorer R (2003) Structural acclimation and radiation regime of silver fir (Abies alba Mill.) shoots along a light gradient. Plant Cell Environ 26(3):429–442

Chmura DJ, Tjoelker MG (2008) Leaf traits in relation to crown development, light interception and growth of elite families of loblolly and slash pine. Tree Physiol 28(5):729–742

Clevers JGPW, Kooistra L, Schaepman ME (2010) Estimating canopy water content using hyperspectral remote sensing data. Int J Appl Earth Obs Geoinf 12(2):119–125

Datt B (1998) Remote sensing of chlorophyll a, chlorophyll b, chlorophyll a + b, and total carotenoid content in eucalyptus leaves. Remote Sens Environ 66(2):111–121

Erdfelder E, Faul F, Buchner A (1996) GPOWER: a general power analysis program. Behav Res Methods Instrum Comput 28(1): 1–11

Fernandes RA, Miller JR, Chen JM, Rubinstein IG (2004) Evaluating image-based estimates of leaf area index in boreal conifer stands over a range of scales using high-resolution CASI imagery. Remote Sens Environ 89(2):200–216

Hallik L, Kull O, Niinemets U, Aan A (2009) Contrasting correlation networks between leaf structure, nitrogen and chlorophyll in herbaceous and woody canopies. Basic Appl Ecol 10(4):309–318

Huber S, Kneubühler M, Psomas A, Itten K, Zimmermann NE (2008) Estimating foliar biochemistry from hyperspectral data in mixed forest canopy. For Ecol Manage 256(3):491–501

Jacquemoud S, Ustin SL, Verdebout J, Schmuck G, Andreoli G, Hosgood B (1996) Estimating leaf biochemistry using the PROSPECT leaf optical properties model. Remote Sens Environ 56(3):194–202

Johnson JD (1984) A rapid technique for estimating total surface area of pine needles. For Sci 30(4):913–921

Kalina J, Urban O, Čajánek M, Kurasová I, Špunda V, Marek MV (2001) Different responses of Norway spruce needles from shaded and exposed crown layers to the prolonged exposure to elevated CO2 studied by various chlorophyll a fluorescence techniques. Photosynthetica 39(3):369–376

Koetz B, Schaepman M, Morsdorf F, Bowyer P, Itten K, Allgöwer B (2004) Radiative transfer modeling within a heterogeneous canopy for estimation of forest fire fuel properties. Remote Sens Environ 92(3):332–344

Kokaly RF, Asner GP, Ollinger SV, Martin ME, Wessman CA (2009) Characterizing canopy biochemistry from imaging spectroscopy and its application to ecosystem studies. Remote Sens Environ 113(Supplement 1):S78–S91

le Maire G, François C, Dufrêne E (2004) Towards universal broad leaf chlorophyll indices using PROSPECT simulated database and hyperspectral reflectance measurements. Remote Sens Environ 89(1):1–28

Lukeš P, Malenovský Z, Hanuš J, Kaplan V, Homolová L, Pokorný R (2009) Challenges in accuracy assessment of Norway spruce leaf chlorophyll content estimated from airborne and satellite imaging spectroscopy data. Workshop on the retrieval of geophysical variables using high spatial resolution optical imagery. ESA/ ESTEC Noordwijk, The Netherlands, 14–15 October 2009

Luyssaert S, Inglima I, Jung M, Richardson AD, Reichstein M, Papale D, Piao SL, Schulze ED, Wingate L, Matteucci G et al (2007) CO2 balance of boreal, temperate, and tropical forests derived from a global database. Glob Change Biol 13(12):2509–2537

Malenovský Z, Ufer C, Lhotaková Z, Clevers JGPW, Schaepman ME, Albrechtová J, Cudlín P (2006) A new hyperspectral index for chlorophyll estimation of a forest canopy: area under curve normalised to maximal band depth between 650–725 nm. EARSeL eProc 5(2):161–172

Moorthy I, Miller JR, Noland TL (2008) Estimating chlorophyll concentration in conifer needles with hyperspectral data: an assessment at the needle and canopy level. Remote Sens Environ 112(6):2824–2838

Morsdorf F, Mårell A, Koetz B, Cassagne N, Pimont F, Rigolot E, Allgöwer B (2010) Discrimination of vegetation strata in a multi-layered Mediterranean forest ecosystem using height and intensity information derived from airborne laser scanning. Remote Sens Environ 114(7):1403–1415

Niinemets Ü (1997) Distribution patterns of foliar carbon and nitrogen as affected by tree dimensions and relative light

conditions in the canopy of Picea abies. Trees Struct Funct 11(3):144–154

Niinemets Ü (2007) Photosynthesis and resource distribution through plant canopies. Plant Cell Environ 30(9):1052–1071

Niinemets Ü (2010) A review of light interception in plant stands from leaf to canopy in different plant functional types and in species with varying shade tolerance. Ecol Res 25:693–714

Niinemets Ü, Kull O (1995) Effects of light availability and tree size on the architecture of assimilative surface in the canopy of Picea abies: variation in needle morphology. Tree Physiol 15(5):307–315

Ollinger SV, Smith ML (2005) Net primary production and canopy nitrogen in a temperate forest landscape: an analysis using imaging spectroscopy, modeling and field data. Ecosystems 8(7):760–778

Palmroth S, Stenberg P, Smolander S, Voipio P, Smolander H (2002) Fertilization has little effect on light-interception efficiency of Picea abies shoots. Tree Physiol 22:1185–1192

Perterer J, Körner C (1990) Das Problem der Bezugsgrösse bei physiologisch-ökologischen Untersuchungen an Koniferennadeln. (The problem of reference parameters in physiologic-ecological research with conifer needles). Forstw Cbl 109(1):220–241

Pokorný R (2002) Index listové plochy v porostech lesních dřevin (Leaf area index of forest canopies). PhD thesis, Mendel University in Brno, Brno, The Czech Republic

Porra RJ, Thompson WA, Kriedemann PE (1989) Determination of accurate extinction coefficients and simultaneous equations for assaying chlorophylls a and b extracted with four different solvents: verification of the concentration of chlorophyll standards by atomic absorption spectroscopy. Biochem Biophys Acta 975:384–394

Rautiainen M, Heiskanen J, Eklundh L, Möttus M, Lukeš P, Stenberg P (2010) Ecological applications of physically based remote sensing methods. Scand J For Res 25(4):325–339

Schlerf M, Atzberger C, Hill J, Buddenbaum H, Werner W, Schüler G (2010) Retrieval of chlorophyll and nitrogen in Norway spruce (Picea abies L. Karst.) using imaging spectroscopy. Int J Appl Earth Obs Geoinf 12(1):17–26

Sellin A (2000) Estimating the needle area from geometric measurements: application of different calculation methods to Norway spruce. Trees Struct Funct 14(4):215–222

Serrano L, Gamon JA, Berry J (1997) Estimation of leaf area with an integrating sphere. Tree Physiol 17(8–9):571–576

Smith WK, Schoettle AW, Cui M (1991) Importance of the method of elaf area measurement to the interpretation of gas exchange of complex shoots. Tree Physiol 8:121–127

Špunda V, Čajánek M, Kalina J, Lachetová I, Šprtová M, Marek MV (1998) Mechanistic differences in utilization of absorbed excitation energy within photosynthetic apparatus of Norway spruce induced by the vertical distribution of photosynthetically active radiation through the tree crown. Plant Sci 133(2):155–165

Stenberg P, Kangas T, Smolander H, Linder S (1999) Shoot structure, canopy openness, and light interception in Norway spruce. Plant Cell Environ 22(9):1133–1142

Svenson SE, Davies FT (1992) Comparison of methods for estimating surface area of water-stressed and fully hydrated pine needle segments for gas exchange analysis. Tree Physiol 10:417–421

Urban O, Janouš D, Acosta M, Czerný R, Marková I, Navrátil M, Pavelka M, Pokorný R, Šprtová M, Zhang R et al (2007) Ecophysiological controls over the net ecosystem exchange of mountain spruce stand. Comparison of the response in direct vs. diffuse solar radiation. Glob Change Biol 13(1):157–168

Ustin SL, Roberts DA, Gamon JA, Asner GP, Green RO (2004) Using imaging spectroscopy to study ecosystem processes and properties. Bioscience 54(6):523–534

Ustin SL, Gitelson AA, Jacquemoud S, Schaepman M, Asner GP, Gamon JA, Zarco-Tejada P (2009) Retrieval of foliar information about plant pigment systems from high resolution spectroscopy. Remote Sens Environ 113:S67–S77

Van der Zande D, Hoet W, Jonckheere I, van Aardt J, Coppin P (2006) Influence of measurement set-up of ground-based LiDAR for derivation of tree structure. Agric For Meteorol 141(2–4):147–160

Waring RH (1983) Estimating forest growth and efficiency in relation to canopy leaf area. Adv Ecol Res 13:327–354

Wellburn AR (1994) The spectral determination of chlorophyll a and chlorophyll b, as well as total carotenoids, using various solvents with spectrophotometers of different resolution. J Plant Physiol 144:307–313

Zarco-Tejada PJ, Miller JR, Harron J, Hu B, Noland TL, Goel N, Mohammed GH, Sampson P (2004) Needle chlorophyll content estimation through model inversion using hyperspectral data from boreal conifer forest canopies. Remote Sens Environ 89(2):189–199